Physics-Informed Neural Networks for Tracking the Hemodynamics of Dissected Aorta

Eric Myzelev, College of Arts and Sciences, Class of 2025

Faculty Mentor: Dr. Lu Lu, Department of Chemical and Biomolecular Engineering

Abstract

Physics informed neural networks (PINNs) have grown from a toy machine learning concept to very powerful and applicable in a variety of modern problems. As PINNs continue to grow, they will inevitably be utilized more in the fields of medicine and biology, where not only are the domains of interest incredibly complex but information on them incomplete. We study PINN performance in the said area via the lens of aortic dissections (AD) informed by MRI scanning. Specifically, we consider the prediction accuracy of PINNs as a function of 4D flow MRI in both spatial and temporal resolutions, and consider PINN prediction of the gradient-based parameter, wall shear stress. Three AD aneurysms are analyzed, those with large, medium and small mouths. These mouths lack any boundary conditions making this an ill-posed problem with standard computational techniques. We utilize PINN aided by 2D MRI data to learn the hemodynamics of the domain. We conclude that full MRI resolution may not be required, saving on scanning cost, and in the case of AD aneurysms, larger mouths lead to more accurate results due to the larger order of magnitude in the velocities which are easier for PINNs to learn.

Introduction

Physics Informed Neural Networks (PINNs) use deep learning to solve partial differential equations (PDEs). In the past few years their popularity has significantly increased due to their ability to solve inverse problems as easily as forward problems. PINNs work by embedding a PDE and its initial/boundary conditions into a neural network's loss function, and then training the network to approximate the PDE's solution.

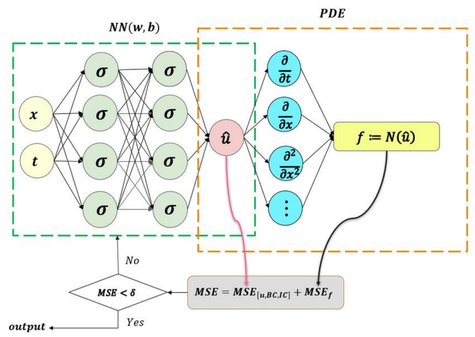

Figure 1. Schematic of PINN.

In the last two decades, computational fluid dynamics (CFD), which simulates blood flow based on Navier-Stokes equations, has been widely employed to illustrate complex blood flow patterns in macro and micro-blood vessels. While the conventional CFD methods can provide 3D high-resolution estimation of the hemodynamics inside patient-specific vessels, the reliability of their predictions accuracy largely depends on the flow boundary conditions for all the involved blood vessels, which may not always available. In addition, CFD simulations entail large memory resources, time-consuming computation and cumbersome preprocessing, such as mesh generation for geometries and boundary condition setup, preventing their deployment to clinic settings.

Objectives

We examine the performance of PINN in predicting hemodynamics in realistic 3D dissected aortas reconstructed from apolipoprotein null mice infused with AngII, a well-established animal model for studying the parthenogenesis and pathology of aortic dissections. We train the PINN on three 4D geometries, representing a small, medium and large aneurysm, respectively. The model is trained using the Navier-Stokes equations and cross-sectional MRI data, and predicts the blood flow velocity v=(u,v,w) and pressure P in the aneurysm. In particular, we aim to demonstrate that PINNs allow us to only focus on assessing the 3D flow field inside the false lumen without modeling the true lumen and various branched vessels, thereby considerably reducing the amount of required measurement data as well as eliminating the dependency of predictions on the accuracy and availability of the boundary conditions. We will also systematically evaluate the model performance on the temporal and spacial resolution of the measurement data (i.e., from 4D MRI), aiming to minimize the data acquisitions while maintaining the adequate accuracy for thrombosis prediction.

Methods

4D flow MRI provides in vivo measurement of blood flow dynamics in blood vessels, or in our case an AD aneurysm. It provides a time-resolved 3D velocity which consists of the magnitude of the velocity and the separate velocity components. Depending on the resolution used by the MRI, the number of slices in a given space may change as well as the number of snapshots - temporal values at which these slices are provided. Here, we explore the impact of changing both spatial and temporal resolution on velocity and WSS prediction. We assume a maximum spatial resolution of 1.5 mm, and a maximum temporal resolution of 30-40 ms. We test the following spatial resolutions: 20%, 40%, 60%, 80%, 100%, and temporal resolutions: 20%, 40%, 60%, 80%, 100%.

We set the loss function of the Neural Network to be

$$\mathcal{L}(\boldsymbol{\theta}) = \mathcal{L}^{pde}(\boldsymbol{\theta}) + \mathcal{L}^{bc}(\boldsymbol{\theta}) + \mathcal{L}^{data}(\boldsymbol{\theta})$$

Where θ represents the model's parameters and observables, and where the PDE loss represents the Navier-Stokes equations:

$$\mathcal{L}^{pde}(\boldsymbol{\theta}) = \sum_{n=1}^{N} w^{pde}(\mathcal{L}_n^{pde_1} + \mathcal{L}_n^{pde_2} + \mathcal{L}_n^{pde_3} + \mathcal{L}_n^{pde_4})$$

$$\mathcal{L}_n^{pde_1} = \frac{1}{N}(\frac{\partial u_n}{\partial x} + \frac{\partial v_n}{\partial y} + \frac{\partial w_n}{\partial z})^2$$

$$\mathcal{L}_n^{pde_2} = \frac{1}{N}(\rho(\frac{\partial u_n}{\partial t} + u_n\frac{\partial u_n}{\partial x} + v_n\frac{\partial u_n}{\partial y} + w_n\frac{\partial u_n}{\partial z}) + \frac{\partial \mathscr{P}}{\partial x} - \mu(\frac{\partial^2 u_n}{\partial x^2} + \frac{\partial^2 u_n}{\partial y^2} + \frac{\partial^2 u_n}{\partial z^2}))^2$$

$$\mathcal{L}_n^{pde_3} = \frac{1}{N}(\rho(\frac{\partial v_n}{\partial t} + u_n\frac{\partial v_n}{\partial x} + v_n\frac{\partial v_n}{\partial y} + w_n\frac{\partial v_n}{\partial z}) + \frac{\partial \mathscr{P}}{\partial y} - \mu(\frac{\partial^2 v_n}{\partial x^2} + \frac{\partial^2 v_n}{\partial y^2} + \frac{\partial^2 v_n}{\partial z^2}))^2$$

$$\mathcal{L}_n^{pde_4} = \frac{1}{N}(\rho(\frac{\partial w_n}{\partial t} + u_n\frac{\partial w_n}{\partial x} + v_n\frac{\partial w_n}{\partial y} + w_n\frac{\partial w_n}{\partial z}) + \frac{\partial \mathscr{P}}{\partial z} - \mu(\frac{\partial^2 w_n}{\partial x^2} + \frac{\partial^2 w_n}{\partial y^2} + \frac{\partial^2 w_n}{\partial z^2}))^2]$$

The loss term for the boundary conditions is

$$\mathcal{L}^{bc}(\boldsymbol{\theta}) = \sum_{b=1}^{N} w^{bc}[\frac{1}{N}(u_n^2 + v_n^2 + w_n^2)]$$

And the data loss is calculated using mean square error.

Results

We begin with a simple prediction, analyzing the medium aneurysm at a medium level of resolution in both spatial and temporal coordinates. Figure 2 depicts 2D slices of the true and predicted velocity for the 60% max spatial and at 60% max temporal resolution. We present the prediction near the center of the mouth at z = 0 for overall velocity and all velocity components, a point that is different from the MRI slices provided, meaning the position we are viewing has not been seen by the neural network in the data loss. The prediction for Figure 2 is at t = 0, a time that we have MRI simulations for and the neural network was able to visualize in the data loss.

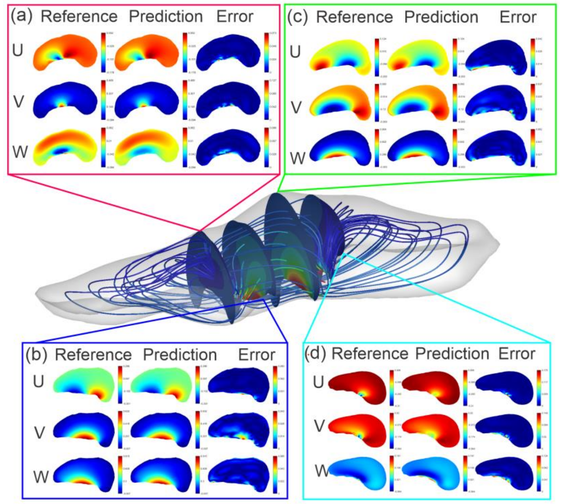

Figure 2: Velocity components for the medium aneurysm at a medium resolution at an observed snapshot.

We note that the overall prediction accuracy is high. It can be seen from the reference solution that there are some eddies being formed in the u and v velocity components. We also note that the general direction of the flow is in the w direction, which is parallel to the flow in the connected artery. As such, the dynamics of w are more straight forward than the other two components. This has two primary effects: the magnitude of w will be much larger than the other two components, and this relationship could change with the size of the mouth; additionally, it also determines where the majority of the error is located. If w is dominant, the PINN will focus on w far more than other components; potentially causing higher relative inaccuracies in the calculation of u and v.

We now look at how L2 error varies as the number of slices and snapshots are varied (Figures 3 and 4). The number of slices represents the spatial resolution, while the number of snapshots represents the temporal resolution. We also run the same tests on a model that does not use the PDE, and instead just predicts using the MRI data. This provides a comparison of our model to a standard deep learning approach. We observe that our model not only outperforms the data-only model at high resolutions, but also experiences significantly lowers drops in accuracy when the resolution is lowered.

Results

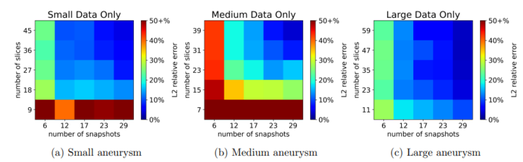

(a) Small aneurysm (b) Medium aneurysm (c) Large aneurysm

Figure 3. L2 Relative Error (a) small, (b) medium, and (c) large aneurysm as a function of MRI Resolution when only data is used for training and no PDE.

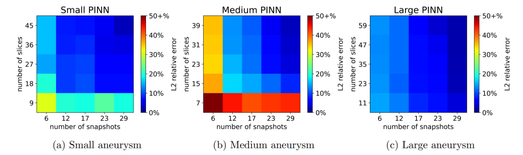

(a) Small aneurysm (b) Medium aneurysm (c) Large aneurysm

Figure 4. L2 Relative Error (a) small, (b) medium, and (c) large aneurysm as a function of MRI Resolution when both the MRI data and the PDE is used for training.

Future Research:
Future work will look at using transfer learning to speed up training and lower computational resources. The model can be first trained on lower resolution data, before the full dataset is introduced.

References

J Ferruzzi, MR Bersi, and JD Humphrey. Biomechanical phenotyping of central arteries in health and disease: advantages of and methods for murine models. *Annals of Biomedical Engineering*, 41:1311–1330, 2013.

Lu Lu, Xuhui Meng, Zhiping Mao, and George E Karniadakis. Deepxde: A deep learning library for solving differential equations. arXiv preprint arXiv:1907.04502, 2019.

Maziar Raissi, Paris Perdikaris, and George E Karniadakis. Physics-informed neural networks: A deep learning framework for solving forward and inverse problems involving nonlinear partial differential equations. *Journal of Computational Physics*, 378:686–707, 2019.

Petter Dyverfeldt, Malenka Bissell, Alex J. Barker, Ann F. Bolger, Carl-Johan Carlh¨all, Tino Ebbers, Christopher J. Francios, Alex Frydrychowicz, Julia Geiger, Daniel Giese, Michael D. Hope, Philip J. Kilner, Sebastian Kozerke, Saul Myerson, Stefan Neubauer, Oliver Wieben, and Michael Markl. 4d flow cardiovascular magnetic resonance consensus statement. *Journal of Cardiovascular Magnetic Resonance*, 17(1), 2015.

Thierry Carrel, Thoralf M Sundt, Yskert von Kodolitsch, and Martin Czerny. Acute aortic dissection. *The Lancet*, 401(10378):773–788, 2023.

Acknowledgements

I would like to extend my deepest gratitude to Dr. Lu Lu for letting me work in his lab in the Department of Chemical and Biomolecular Engineering in the School of Engineering and Applied Sciences. I would also like to thank Mitchell Daneker for providing me guidance throughout the project. Lastly, I would like to thank the University of Pennsylvania and the Grants for Faculty Mentoring Undergraduate Research (GfFMUR) program for funding and supporting this project.